



Continuous Wavelet Transform and Dynamic Time Warping-Based Fine Division and Correlation of Glutenite Sedimentary Cycles

Zhichao Yu¹ · Zhizhang Wang¹ · Jie Wang²

Received: 14 January 2022 / Accepted: 18 November 2022 / Published online: 16 December 2022
© International Association for Mathematical Geosciences 2022

Abstract

Glutenite reservoirs are characterized by strong heterogeneity, large thickness, complex rock fabric, and low maturity in terms of structure and composition, which makes the division of sedimentary periods an arduous task. This restricts the exploration and development of oil and gas fields in glutenite reservoirs. Wireline logging signals, which contain rich geological information and record the sedimentary cycle of the strata, are sensitive to changes in the lithologic interface. Moreover, the formation microscanner image (FMI) method provides a complete lithologic profile of the formation and intuitively identifies sequence boundaries, unlike cores and conventional well logs. By integrating mathematical tools based on time–frequency analysis technology of multiscale wavelet transform and FMI as the geological constraint, a sensitive logging curve was selected to delineate the sedimentary cycles of a glutenite reservoir. Optimization of wavelet decomposition parameters was conducted by employing Morlet as the wavelet base, and the scale factors were screened by the direct power spectrum method. Taking the glutenite reservoirs of the Baikouquan Formation in the MA131 well block of the Mahu Sag as the research object, the sedimentary periods of the glutenite body of well MA15 were divided under seismic constraints. The results indicated that the abrupt interface of the wavelet coefficient curve of different scale factors closely corresponded to the interface of sedimentary cycles at distinct levels. This demonstrates the effectiveness of the proposed method. Subsequently, the dynamic time warping algorithm was employed for automatic stratigraphic well correlation. It is concluded that the proposed technique eliminates the overdependence on traditional methods, such as geological and well stratification information, as well as possessing superiority with regard to high precision, better flexibility, and convenient operation.

✉ Zhizhang Wang
wang_zhizhang@126.com

¹ College of Geosciences, China University of Petroleum, Beijing 102249, China

² CNOOC China Limited, Shenzhen Branch, Shenzhen 518064, Guangdong, China

Keywords Sedimentary period · Wavelet transform · Glutenite reservoir · Dynamic time warping

1 Introduction

As the exploration and development of unconventional oil and gas reservoirs increases, countries all over the world have gradually considered unconventional oil and gas resources as one of the primary objectives of energy utilization (Hosseini et al. 2021; Wachtmeister et al. 2020; Fangzheng 2019; Yu et al. 2021, 2022). Glutenite is a relatively common type of unconventional tight oil and gas reservoir that is present in a number of petroliferous basins around the world with abundant oil and gas resources (Song et al. 2020; Liu et al. 2022a, b; Liu et al. 2022a, b). In addition, glutenite is generally formed in a sedimentary environment that is characterized by rapid accumulation, causing complex lithology, varying thickness, diverse diagenesis, and low structural and compositional maturity (Wu et al. 2020; Xi et al. 2021). Currently, studies on glutenite are mostly focused on sedimentary characteristics, reservoir characteristics, reservoir evaluation, and hydrocarbon accumulation mechanisms (Qin et al. 2020; Li et al. 2020). Moreover, delineating sedimentary periods is the key process in stratigraphic framework establishment, as well as the foundation for later exploration and exploitation. The common sets of data employed to detect geological sequence boundaries include cores, as well as palaeontological, palaeomagnetic, geochemical, and geophysical data (Cross et al. 1993). In particular, these datasets play an important role in the identification and correlation of stratigraphic units. Over the past few decades, several approaches have been proposed to detect geological boundaries from the above dataset. For instance, to improve the ability to identify sequence boundaries, MacEachern and Pemberton (2002) employed relict fossil sequences and relict facies data in the study of genetic strata. Using palaeontological data, the variation in the degree of magnetic clastic particle concentration caused by climate change and global sea-level fluctuation was applied to a stratigraphic division of deep marine sedimentary carbonate strata (Nio 2005). As the most direct geological data, cores can be used to determine the sedimentary period interface more intuitively. Nevertheless, cored wells are generally limited due to the high cost of coring. Furthermore, geophysical data, such as seismic and wireline logs, have been implemented by many researchers for the subdivision of stratigraphic units (Guo et al. 2021; Teixeira et al. 2020; Mianaekere et al. 2020). Despite the significant role of seismic data in the identification of sequence boundaries, it can be used only to divide low-order sequences due to its relatively low resolution. Therefore, well logs are preferable data sources for stratigraphic subdivisions due to their availability. There are excellent cases in the literature in which sequence divisions are carried out, usually manually, by employing different wireline logs (Liang et al. 2019; Wang et al. 2020). The results of manual interpretation depend highly on the experience of the interpreter, which may lead to multiple detections of sequence boundaries (Rivera Vega 2004; Perez-Muñoz et al. 2013). Moreover, the dynamic time warping (DTW) algorithm has been used in the past to correlate logs. Baville et al. (2022) proposed an approach that translates sedimentary concepts into a correlation cost, which is utilized to populate a cost matrix

to apply DTW for stratigraphic correlation. Behdad (2019) constructed spectral trend logs, wherein DTW was subsequently used for automatic stratigraphic correlation. In addition to the aforementioned methods, other signal processing techniques have been implemented to analyse well logs, including Fourier transform (Weedon 2003), principal component analysis (Karimi et al. 2021), and wavelet transform (Behdad 2019). These methods are pure mathematical analyses with no geological constraints. Due to the paucity of biological fossils, stratification marks in the wireline logging response are not visible during a sedimentation event of thick glutenite (Qing et al. 2020). Thus, the division of sedimentary periods is quite difficult, and this severely affects the characterization of the internal reservoir structure of the glutenite body. This has become one of the bottlenecks restricting the exploration of glutenite reservoirs.

The tight conglomerate reservoirs in the Mahu oilfield were deposited in a fluvial fan delta sedimentary system, with rapid accumulation near the provenance. Although there are many appraisal wells in the MA131 well block, the drilling and well test results have shown low economic efficiency because of the strong heterogeneity of the reservoirs. The sediments feature the superposition of multiple sedimentary cycles, which are recorded in the wireline logging sequence obtained from a single well.

The purpose of this paper is to provide a novel method for dividing sedimentary periods and well correlations that incorporates mathematical tools and geological knowledge. First, the identification of sequence boundaries was performed using wireline logs via continuous wavelet transform under the constraints of three-dimensional seismic data, while the formation microscanner image (FMI) was employed to validate the effectiveness of the method. Afterwards, DTW was applied to correlate wells to lay a foundation for subsequent well deployment and efficient development of the glutenite reservoir in the study area.

2 Methodology and Workflow

2.1 Continuous Wavelet Transform

The concept of wavelet transform is to combine a cluster of mother wavelets $\psi(t)$ to approximate the signal $f(t)$ via translations and dilatations (Fig. 1). In comparison with the Fourier transform and short-time Fourier transform (STFT), the wavelet transform has better time–frequency locality. It overcomes the limitation of a fixed window of

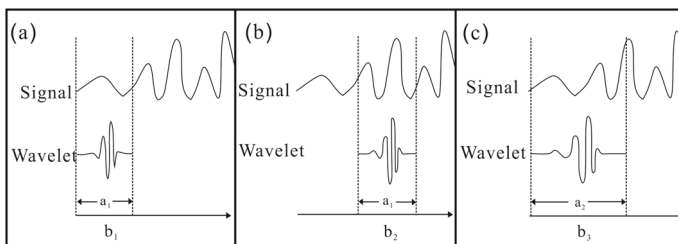


Fig. 1 Schematic diagram of a continuous wavelet transform

STFT and achieves rapport in the time–frequency domain through the scaling and translation of the wavelet function, ultimately achieving the corresponding accuracy at different positions of the signal (Shi et al. 2022). The continuous wavelet transform function $WT_f(a, b)$ is defined as

$$WT_f(a, b) = \left| a^{\frac{1}{2}} \right| \int_{-\infty}^{\infty} f(t) \psi\left(\frac{t-b}{a}\right) dt \quad a \neq 0, \quad (1)$$

where $WT_f(a, b)$ is the function of parameters a and b . The steps to obtain the function are as follows:

- (1) Select the wavelet with fixed wavelength a_1 and compare it with the beginning of the original signal $f(t)$.
- (2) Calculate $WT_f(a, b)$, as shown in Fig. 1a. It represents the correlation degree between the starting segment of signal $f(t)$ and the selected mother wavelet. The larger $WT_f(a, b)$ is, the more similar they are. The result depends on the shape of the selected mother wavelet.
- (3) Shift the mother wavelet to the right and repeat steps 1 and 2, as shown in Fig. 1b, until all signals are processed.
- (4) Stretch the mother wavelet from a_1 to a_2 , and repeat steps 1 to 3, as shown in Fig. 1c.
- (5) Repeat steps 1 to 4 for all wavelet transform scales to obtain all the $WT_f(a, b)$.

2.2 Dynamic Time Warping

There are many distance functions in time series data, with the most prominent being DTW (Hung et al. 2022). Since DTW was first proposed by Itakura (1975) in the 1970s, it has been widely applied in many fields. The time warping function $W(n)$ satisfying certain conditions is employed to describe the temporal correspondence between the test template and the reference template for the solution of the minimum cumulative distance given two matched templates. The test series shares i frame vectors, while the reference template has j frame vectors ($i \neq j$). The time warping function $j = W(i)$, which nonlinearly maps the time axis i of the test vector to the time axis j of the template, remains to be solved such that the function $W(i)$ meets the minimum total distance between all the frame vectors. The implementation of DTW is described as follows (Fig. 2): given two time series Q and C , with lengths n and m , respectively, a matrix grid of $n \times m$ is constructed to align the two sequences. The matrix element (i, j) represents the distance $d(q_i, c_j)$ between q_i and c_j (that is, the similarity between each point of sequence Q and each point of C ; the smaller the distance, the higher the similarity). The algorithm can be summed to determine a minimum path through several grid points. The minimum path through which the curve passes consists of the aligned points of the two sequences.

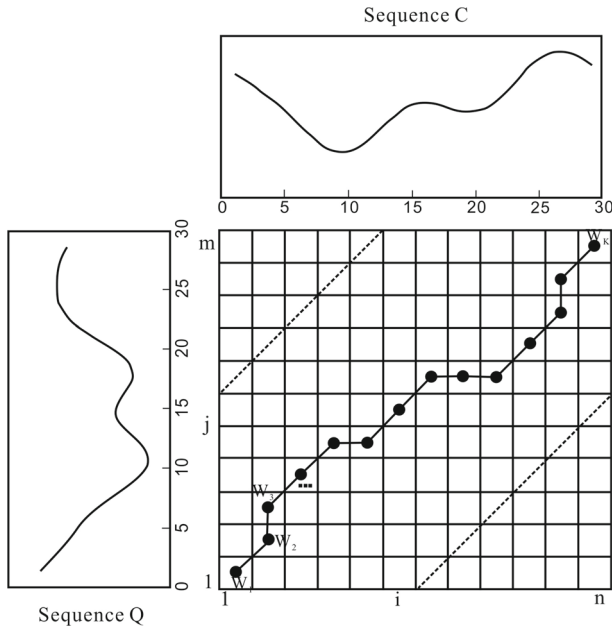


Fig. 2 Schematic diagram of dynamic time warping. W is the warping path. The k th element of W is defined as $W_k = (i, j)_k$, which defines the mapping of sequences Q and C

2.3 Description of the Implemented Approach

As one of the most popular time–frequency analysis methods, wavelet transform can convert logging curves into a depth–frequency domain. In this paper, wavelet transform is utilized to help divide stratigraphic sequences by using wireline logs, which contain stratigraphic information, including the lithology, thickness and location of the sequence boundary. Afterwards, the DTW algorithm, in which the standard well is selected as the reference well and other wells are considered observation wells, was proposed to perform the well-to-well correlation process. Wireline log data are the primary input data required for the experiment. Moreover, depths of geological boundaries in the reference well must be available to enable the DTW algorithm to detect similar boundary information in other wells.

First, a stratigraphy forwards model is established to validate the effectiveness of the proposed method. Then, the reference well that contains FMI images is determined by accurately dividing the sedimentary periods under seismic constraints through micro-resistivity scanning images and well logs. The selection of the wavelet base is predominantly determined by applying time–frequency analysis in the simulated cycle signal with different mother wavelets. Afterwards, the scale factors are screened by the direct power spectrum method. Thus, the sedimentary period can be divided by extracting the corresponding coefficient curves at different scales, while the interfaces of strata can be identified as abrupt points. Finally, the DTW algorithm was employed

for automatic well correlation under the fifth-order sequence (sand group) boundary constraint.

3 Results and Discussion

3.1 Verification of Ideal Sequence Stratigraphic Model

Following the characteristics of grain size successions in sedimentary rocks, the stratigraphic sequence can be classified into the following three basic types: retrogradation, progradation, and aggradation. Thus, three ideal stratigraphic sequence models were established (Fig. 3a, d and g). A retrogradation model is a positive cycle, where the thickness of the conglomerate thickens as the burial depth increases, and the ratio of gravel to mud increases downwards. This indicates that from deep to shallow locations in the sequence, the sediment particle size varies from coarse to fine, and the hydrodynamic force gradually decreases. In contrast, a progradation model is a reverse cycle, which has the opposite characteristic as that of the retrogradation model. The third model is the aggradation model, in which the conglomerate thickness remains unchanged within the burial depth, as well as the ratio of gravel to mud. This result reflects a relatively stable sedimentary environment and hydrodynamic conditions. These three models represent three basic parasequence sets: retrogradational, progradational, and aggradational. The forward model used a Morlet wavelet with a sampling rate of 1,024 Hz.

On the time–frequency spectrum map (Fig. 3b, e, h), the local energy gobbet of the retrogradation formation model gradually weakens with increasing depth and moves towards a small scale (high frequency), while the progradation formation model gradually increases and moves towards a large scale (low frequency). The local energy gobbet of the aggradation formation model does not change significantly with depth and is relatively stable. With regard to the wavelet coefficient diagram (Fig. 3c, f, i), the amplitude and frequency of the retrogradation model gradually decrease as burial depth increases, whereas the amplitude and frequency of the progradation model show an increasing trend. The amplitude and frequency of the aggradation model do not change with depth. The peak and trough of each wavelet coefficient curve correspond to mudstone and conglomerate intervals, respectively. Furthermore, the lithologic mutation interface corresponds to the peak and trough conversion points. The following principles can be summarized based on the aforementioned analysis: The movement of the local energy gobbet with depth reflects the rhythmic characteristics of sediment particle size and hydrodynamic conditions. It can be further employed to analyse formation cyclicality. The crest or trough of the corresponding wavelet coefficient curve can be considered a stratigraphic abrupt boundary, corresponding to the sedimentary intermittent surface or denudation interface of the geological body. Therefore, it can reflect a change in the sedimentary environment.

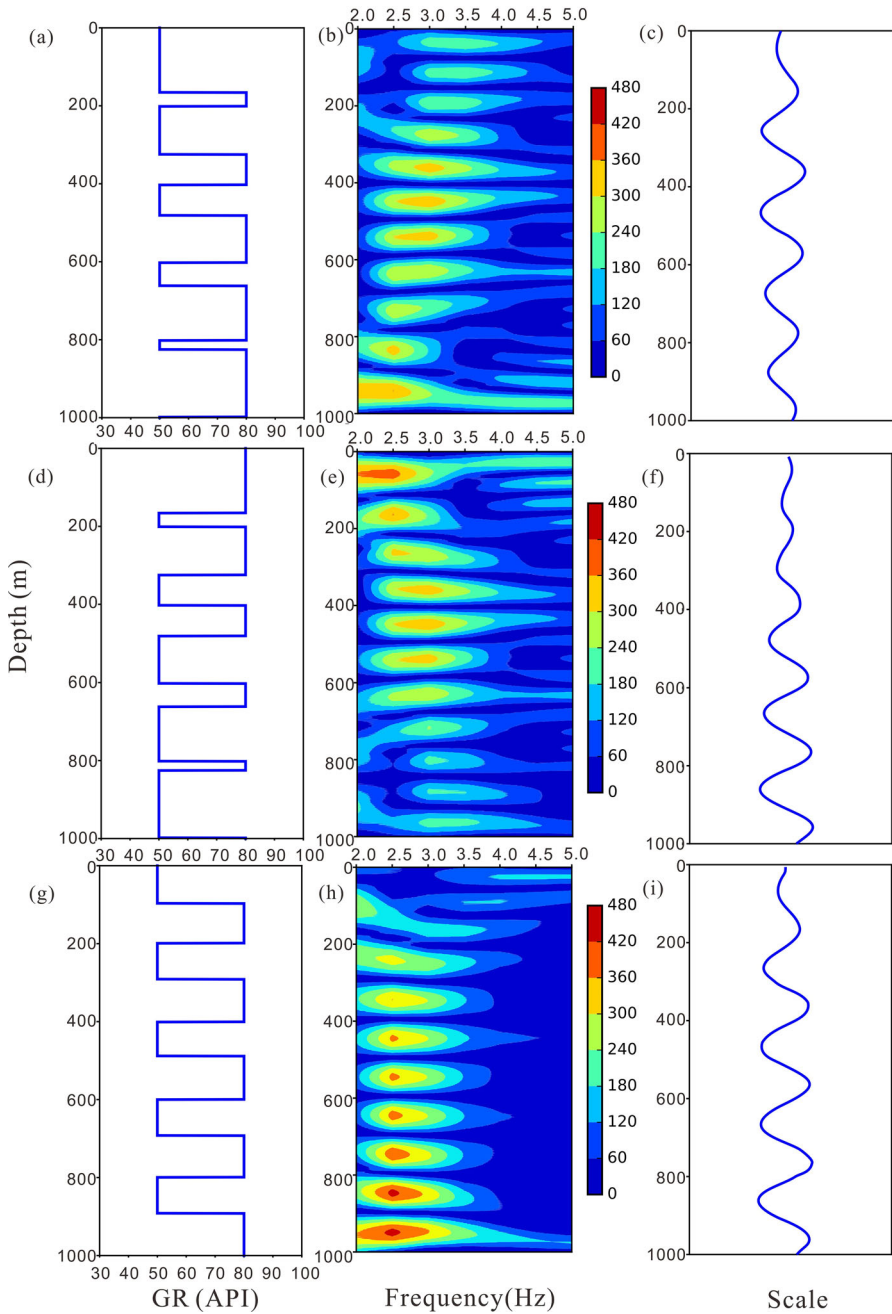


Fig. 3 A forward stratigraphic model used to verify the effectiveness of the proposed method. **a**, **d**, and **g** represent the retrogradational, progradational, and aggradational stratigraphic model, respectively; **b**, **e**, and **h** exhibit the time–frequency map of the related stratigraphic model; **c**, **f**, and **i** are the wavelet coefficient curves extracted after wavelet transform

3.2 Optimization of Wavelet Decomposition Parameters

3.2.1 Selection of an Optimum Mother Wavelet

There are numerous mother wavelet functions that can be employed for continuous wavelet transforms. In addition to Morlet, Mexh, Shan, Gauss, and other wavelets provided by MATLAB (Higham et al. 2016), there are many wavelets built by researchers in processing actual data. Wavelet transform is greatly affected by the original signal and mother wavelet function. The more similar the wavelet is to the signal, the higher the accuracy of compression, denoising, and frequency division. Hence, a thorough examination of the time–frequency focusing property of different mother wavelets, such as vanishing moment and orthogonality, is required when performing wavelet analysis on real data, thus allowing the selection of the best mother wavelet. Moreover, a reasonable criterion for choosing a mother wavelet basically consists of two aspects: the first is its time–frequency locality, that is, the quality of time–frequency accuracy; the second is the resemblance between the mother wavelet and the original signal, where the higher the resemblance, the more accurate the result of the analysis.

Therefore, we intend to use a composite cosine signal to simulate the logging curve and its periodic characteristics with the following formula: $(t) = \cos(2\pi t) + \cos(8\pi t) + \cos(20\pi t) + \cos(40\pi t)$. The waveform diagram of the signal and its components are depicted in Fig. 4. The signal is made up of four components with respective dominant frequencies of 1 Hz, 4 Hz, 10 Hz, and 20 Hz.

Figure 5 illustrates the time–frequency spectrum and the reconstructed primary scale (1 Hz component) after wavelet transform of analogue signals with different mother wavelets. By comparing the diagrams, it is obvious that the wavelet transform using the Mexh wavelet possesses inadequate time–frequency accuracy, owing to the confusing reconstruction of the primary scale. Moreover, the Shan wavelet and the Cgau wavelet have considerable high-frequency jitter in the time–frequency spectrum. The Morlet wavelet has superior time–frequency precision, and the reconstructed main scale is closer to 1 Hz. Thus, the Morlet mother wavelet is chosen for future investigation.

3.2.2 Finding Proper Wavelet Transform Decomposition Levels

Consider a nonstationary signal $z(t) = \sin(2\pi t) + \sin(8\pi t(t < 1 \text{ or } t > 4)) + \sin(20\pi t(1.5 < t < 3.5)) + \sin(40\pi t)$, with dominant frequencies of 1 Hz, 4 Hz, 10 Hz and 20 Hz. Moreover, noticeable sedimentary discontinuities are encountered at $t = 1$ s, 1.5 s, 3.5 s, and 4 s (as shown in Fig. 6). Morlet wavelet transform is performed on the above signal, and the time–frequency spectrum is presented in Fig. 7.

It can be concluded that the wavelet transform can clearly identify four frequency components in the time–frequency spectrum. The direct power spectrum method, which is defined as the signal power in a unit frequency band, is used to establish a strategy to precisely identify the appropriate decomposition level. It depicts the variation in signal power with frequency, that is, the distribution of signal power in the frequency domain. As shown in Fig. 8, the scale (frequency) corresponding to the extremum of the curve is the principal scale component of the original signal.

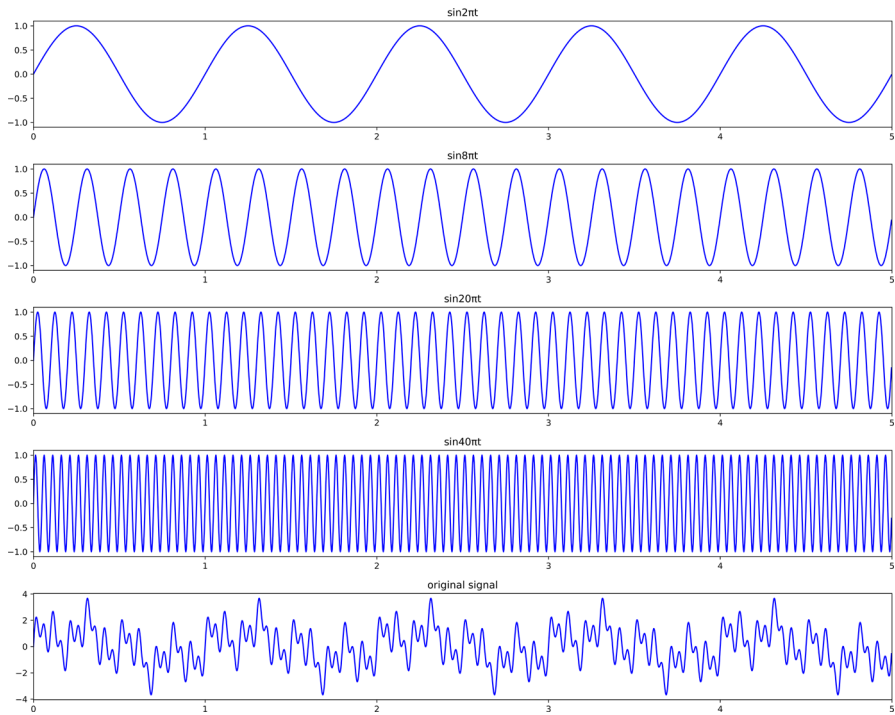


Fig. 4 Simulating signal and its components

The 1.011, 4.044, 9.958, and 19.92 Hz signals identified by this method are basically consistent with 1, 4, 10, and 20 Hz, which confirms the ability of this method to correctly determine the decomposition levels.

3.3 Division and Correlation of the Sedimentary Cycle

As the most direct geological data, cores are used to intuitively identify lithology, sedimentary structures, and sequence boundaries, such as typical lithologic mutation interfaces and scouring surfaces. However, due to the high cost of coring, a thorough study of the sedimentary stage via core observation is not practical. In contrast to coring and conventional well logging, the FMI method can provide a complete formation lithologic profile, as well as more accurate information in revealing sedimentary sequences (Fan et al. 2021; Teama et al. 2018). Figure 9 shows the FMI image interval of well MA15 in the research region where sequence boundaries such as scouring interfaces and lithologic mutation boundaries are recorded. The particle size gradually decreases upwards until the transition to the mudstone interval with horizontal bedding at the top, constituting the basic sedimentary cycle unit. Multiple fundamental sedimentary units of such an ordered combination overlap vertically, forming a higher-order stratigraphic sequence.

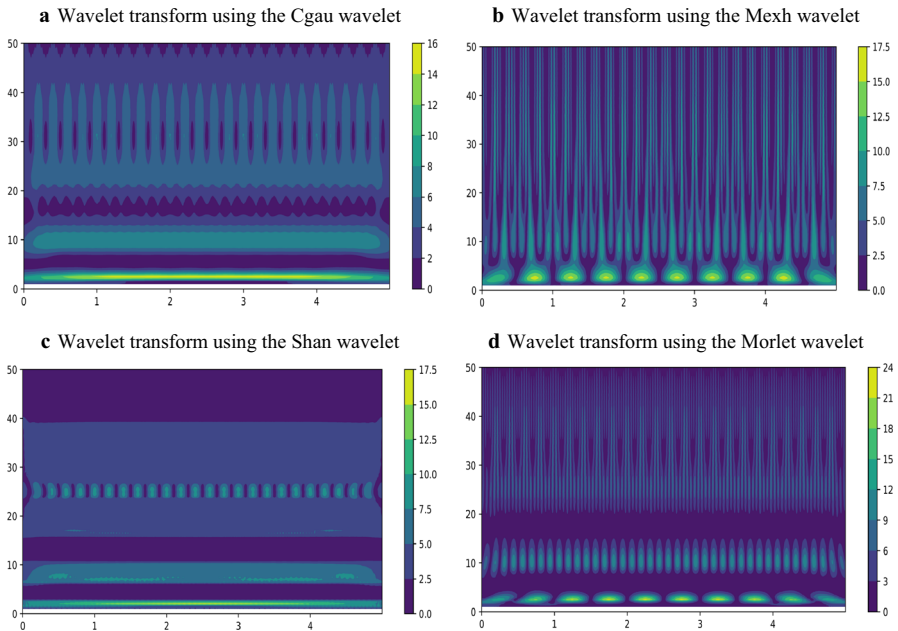


Fig. 5 Reconstructed component with different mother wavelets after wavelet transform

Based on the examination of well log responses for distinct lithologies, implementing deep resistivity (RT) logs resulted in better prediction of the boundary depth in the studied wells (Fig. 10). In other words, this log is the most relevant for our investigation and can provide information about geological boundaries. The time–frequency spectrum was obtained using a one-dimensional continuous wavelet transform on the RT curve of well MA15. Moreover, the decomposition level with the associated sequence order was determined using the direct power spectrum approach. The wavelet transform scales 376 and 1,018 identified by the power spectrum correspond to the fourth and fifth sequence orders, respectively (Fig. 9).

Therefore, the sedimentary cycle division can be carried out through the wavelet transform coefficient curve by integrating the near-well seismic trace and RT time–frequency spectrum. There are two obvious periodic cycle interfaces that can be observed via FMI. Matching the two wave troughs of the curve with a scale of 1,018 corresponds well with the fourth-order sequence boundary. Moreover, the wavelet coefficient curve with a scale of 376 can provide higher-order sequence boundary identification than seismic data (Fig. 9). The wave crest or trough of the wavelet coefficient curve matched perfectly with the sequence boundary identified by the FMI and reflected the changing trend of the local energy gobblet exhibited in the time–frequency spectrum.

Subsequently, the DTW algorithm was employed for automatic well correlation between wells MA15 and MA155 (Fig. 11). The most important output of DTW, the warping path, was employed to connect the two wells (Fig. 12). In addition, we

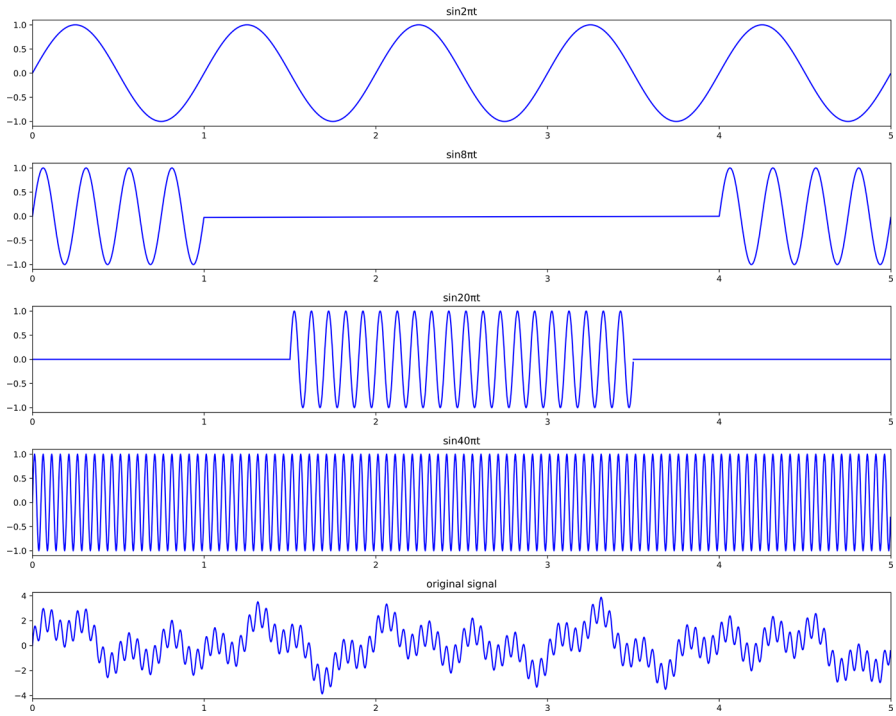


Fig. 6 A nonstationary signal and its components

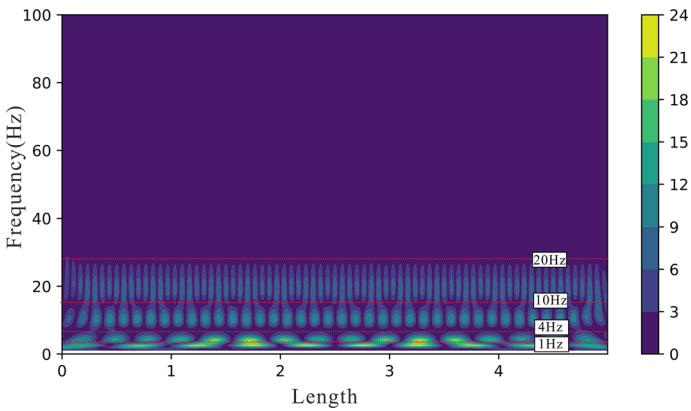


Fig. 7 Time–frequency spectrum of the simulated signal. The four frequency components were identified in the time–frequency spectrum

Fig. 8 Power spectrum of the simulated signal. A plot magnifying the range of 0 to 25 Hz is shown on the right

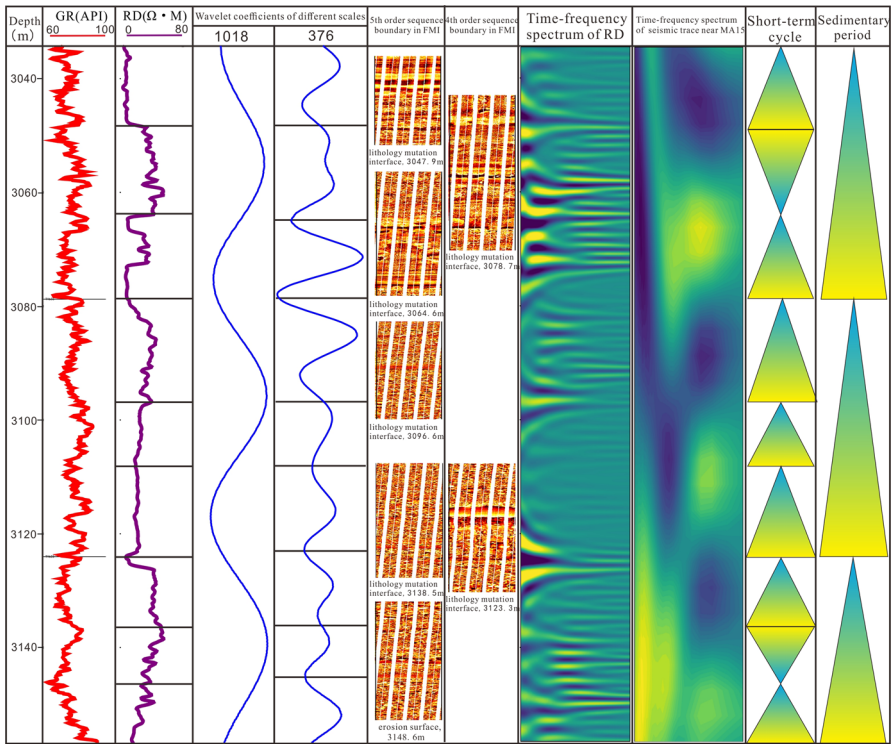
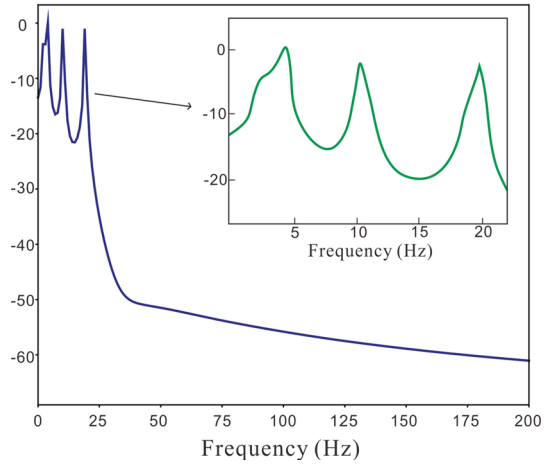


Fig. 9 Stratigraphic sequence subdivision of reference well MA15

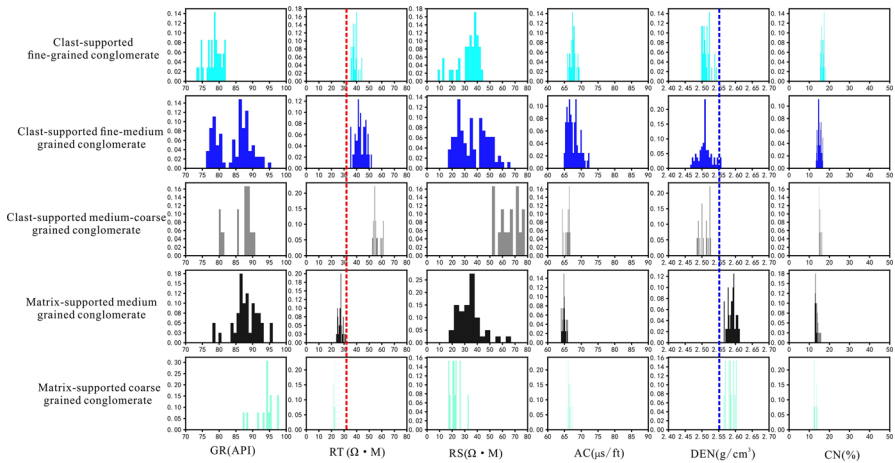


Fig. 10 Conventional well logging characteristics of distinct lithofacies in the study area

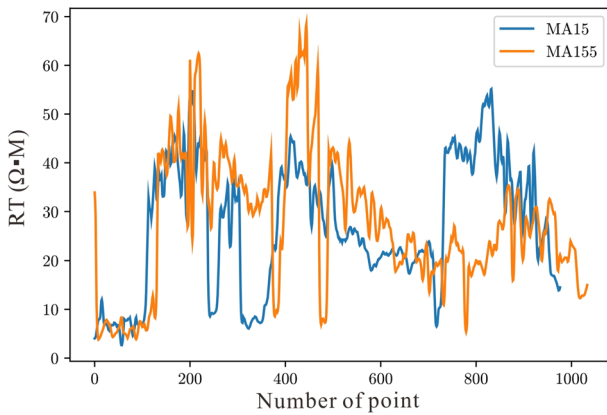


Fig. 11 Original RT curves of reference well MA15 and well MA155

have addressed the issue when a sand interval is missing. The RT curve of the conglomerate interval between 3,160 and 3,170 m was assumed to be missing in well MA155 (Fig. 13). Then, the DTW algorithm was applied for automatic well correlation between wells MA155 and MA15 (Fig. 14). It was discovered that the warping path was the same as the output shown in Fig. 12 before the missing interval was encountered. However, the aligned points were totally different in the subsequent depth interval. Therefore, the application of DTW needs to be improved in future work under such circumstances. Herein, the strata of the Baikouquan Formation are completely preserved, with no sedimentary hiatuses. Theoretically, the reference well can be correlated with the second well by applying the warping path. However, while a reference table of correlation between the reference well and the corresponding second well was employed for high-resolution correlation, there could be more than 50

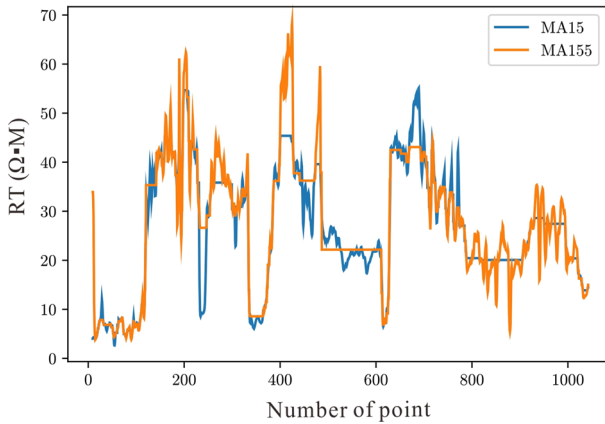


Fig. 12 Warped RT from two wells

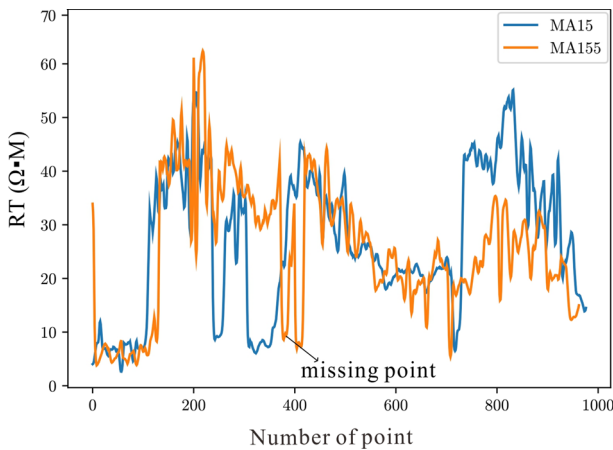


Fig. 13 Missing RT of well MA155 and complete RT of well MA15

possible correlation lines in this research (Fig. 15). The results indicated that the resolution of the correlation was noticeably improved and could help correlate not only the fourth- or fifth-order sequence boundary but also the layering inside the reservoir. Nonetheless, in the early stage of oilfield exploration, the primary concern is to accurately identify the fifth-order sequence boundary for the establishment of a sequence framework and the deployment of exploration wells, rather than the layer division for later exploitation, which is a difficult task that requires much effort if the geology is complex. Herein, the fifth-order sequence boundary of the reference well MA15 is calibrated by FMI. Therefore, the corresponding aligned point of the second well can be located via this approach.

Following this principle, the well correlation under the fifth-order sequence boundary constraint was performed in all the wells along the provenance direction to

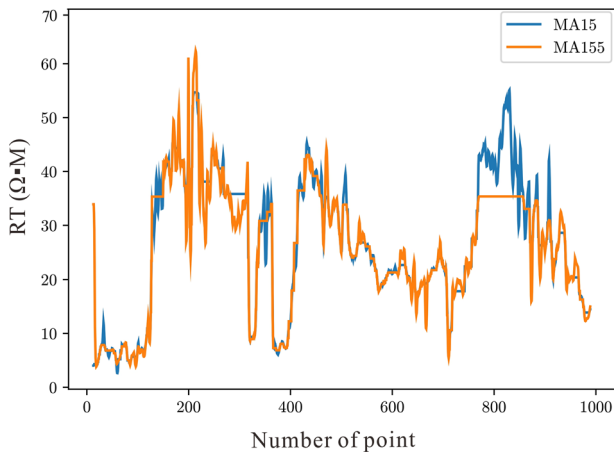


Fig. 14 Warped RT of the two curves in Fig. 13

construct the stratigraphic sequence framework (Fig. 16a). The results indicated that the sequence boundaries are the conversion points of the local energy gobbet on the time–frequency spectrum maps. Afterwards, the sedimentary microfacies were interpreted on the basis of their logging response under the constraint of the stratigraphic framework. It can be concluded that the fan delta front facies are widely developed throughout the whole region, predominantly comprising underwater distributary channels, mouth bars, and sandy debris flows. From T_1b_1 to T_1b_3 , the retrograded fan deltaic depositional system was created in the process of lake transgression (Fig. 16b, c, d). The favourable facies belt in the study area is the underwater distributary channel in T_1b_{21} (Fig. 16c), where long horizontal wells could be deployed to enhance the estimated ultimate recovery of a single well for the production development of tight oil reservoirs.

4 Conclusions

In this study, the division and correlation of glutenite sedimentary cycles are presented based on wavelet transform and DTW under seismic and FMI constraints. By constructing ideal sequence stratigraphic models, the responses of the sequence boundary on the wavelet coefficient curve and time–frequency spectrum were analysed. To determine the optimal mother wavelet and decomposition level, a composite cosine signal was built to simulate the logging curve and its periodic characteristics. The results showed that the Morlet wavelet, of which the reconstructed principal scale was the closest to the original signal, had the highest time–frequency accuracy. Moreover, the power spectrum method was adopted to validate the effectiveness and accuracy for the determination of the optimal decomposition level.

The analysis of well log responses for different lithologies indicated that RT was the most appropriate curve for providing the geological boundary information in our

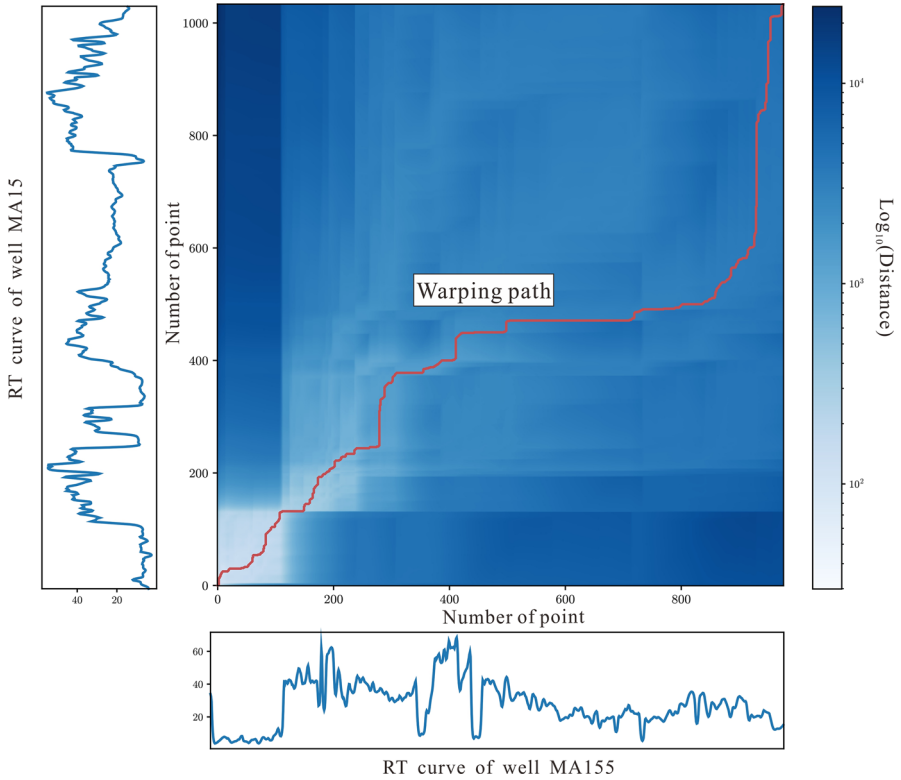


Fig. 15 Warping path from two wells

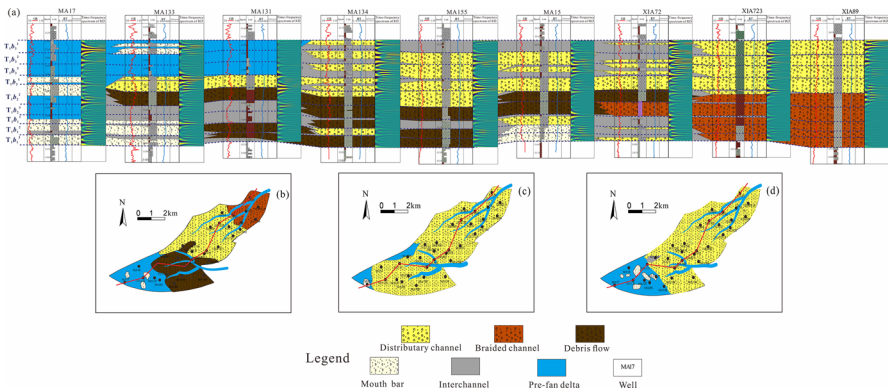


Fig. 16 a Well correlation under the fifth-order sequence boundary constraint throughout all the wells along the provenance direction; b, c, and d are the deposition maps of sand groups $T_{1b_1}^1$, $T_{1b_2}^1$, and $T_{1b_3}^2$, respectively

research. The sedimentary cycle division was carried out through the wavelet transform coefficient curve and time–frequency spectrum under seismic and FMI constraints. The wave crest or trough of the wavelet coefficient curve matches well with the sequence boundary identified by the FMI and reflects the changing trend of the local energy goblet exhibited on the time–frequency spectrum maps. Subsequently, the DTW algorithm was employed for automatic well correlation. The fifth-order sequence boundary of reference well MA15 was calibrated by FMI. Consequently, the well correlation under the fifth-order sequence boundary constraint was performed throughout all the wells along the provenance direction to construct the stratigraphic sequence framework.

The method proposed in this paper was applied to a real case study from a Chinese oilfield. The results demonstrated that the proposed method is capable of sedimentary cycle division and automated well-to-well correlation. Integrating FMI and logging curve data with mathematical tools eliminates the overdependence on traditional methods, such as geological information. Furthermore, a combination of the aforementioned dataset and mathematical tools is superior with regard to high precision, better flexibility, and convenient operation. Of note, this approach, like other mathematical methods, will need to be validated and constrained by other supplementary data that can provide geological sequence boundary evidence, such as biostratigraphy, climate stratigraphy, sequence, and seismic stratigraphy.

Acknowledgements This study was supported by the Strategic Cooperation Technology Projects of CNPC and CUPB (Grant No. ZLZX2020-01). We are deeply grateful to the Exploration and Development Research Institute of Xinjiang Oilfield, CNPC, for providing research data and publication permission. We thank the Editor and anonymous reviewers for their thorough and critical reviews and suggestions, which have significantly improved the quality of this paper.

Author's Contribution ZY: Conceptualization, Methodology, Writing—original draft, Writing-review and editing. ZW: Project administration, Supervision. JW: Formal analysis.

Declarations

Conflict of interest The authors declare that they have no known competing financial interests or personal relationships that could have appeared to influence the work reported in this paper.

References

- Baville P, Apel M, Hoth S, Knaust D, Antoine C, Carpentier C, Caumon G (2022) Computer-assisted stochastic multi-well correlation: Sedimentary facies versus well distality. *Mar Pet Geol* 135:105371. <https://doi.org/10.1016/j.marpetgeo.2021.105371>
- Behdad A (2019) A step toward the practical stratigraphic automatic correlation of well logs using continuous wavelet transform and dynamic time warping technique. *J Appl Geophys* 167:26–32. <https://doi.org/10.1016/j.jappgeo.2019.05.007>
- Cross T, Baker M, Chapin M, Clark M, Gardner M, Hanson M, Lessenger M, Little L, McDonough K, Sonnenfeld M (1993) Applications of high-resolution sequence stratigraphy to reservoir analysis. *Collect Colloq Et Seminaires-Institut Francais Du Petrole* 51:11–33
- Fan H, Shi J, Fan T, Gao Z, Gu Y, Gao Z, Zhang T, Li Y, Li B (2021) Sedimentary microfacies analysis of carbonate formation based on FMI and conventional logs: a case study from the Ordovician in the Tahe Oilfield, Tarim Basin, China. *J Pet Sci Eng*. <https://doi.org/10.1016/j.petrol.2021.108603>
- Fangzheng J (2019) Re-recognition of “unconventional” in unconventional oil and gas. *Pet Explor Dev* 46(5):803–810

- Guo W (2021) Influence of sediment supply rate on sequence stratigraphic architecture change: a case study from the Kaiping Sag, northern South China Sea. *Mar Pet Geol.* <https://doi.org/10.1016/j.marpetgeo.2021.105106>
- Higham DJ, Higham NJ (2016) *MATLAB guide*. Siam, New Delhi
- Hosseini SH, Hamed SG, Kazemi A (2021) Oil price future regarding unconventional oil production and its near-term deployment: a system dynamics approach. *Energy.* <https://doi.org/10.1016/j.energy.2021.119878>
- Hung L-C, Ya-Han Hu, Tsai C-F, Huang M-W (2022) A dynamic time warping approach for handling class imbalanced medical datasets with missing values: a case study of protein localization site prediction. *Expert Syst Appl.* <https://doi.org/10.1016/j.eswa.2021.116437>
- Itakura F (1975) Minimum prediction residual principle applied to speech recognition. *IEEE Trans Acoust Speech Signal Process* 23:67–72
- Jianhua Q, Jing Z, Qingping J (2020) Sweet spot classification evaluation of tight conglomerate reservoir in Mahu sag and its engineering application. *China Pet Explor* 25(02):110–119
- Karimi AM, Sadeghnejad S, Rezghi M (2021) Well-to-well correlation and identifying lithological boundaries by principal component analysis of well-logs. *Comput Geosci.* <https://doi.org/10.1016/j.cageo.2021.104942>
- Li G, Qin J, Xian C (2020) Theoretical understandings, key technologies and practices of tight conglomerate oilfield efficient development: a case study of the Mahu oilfield, Junggar Basin, NW China. *Pet Explor Dev* 47(6):1185–1197
- Liang J, Wang H, Blum MJ, Ji X (2019) Demarcation and correlation of stratigraphic sequences using wavelet and Hilbert-Huang transforms: A case study from Niger Delta Basin. *J Pet Sci Eng.* <https://doi.org/10.1016/j.petrol.2019.106329>
- Liu J, Ge H, Mou S, Wang X, Wang J (2022a) Characterization of meso-structure of glutenite reservoirs by ultrasonic characteristics and the velocity heterogeneity. *J Pet Sci Eng.* <https://doi.org/10.1016/j.petrol.2021.109436>
- Liu J, Ge H, Zhang Z, Wang X, Wang J (2022b) Influence of mechanical contrast between the matrix and gravel on fracture propagation of glutenite. *J Pet Sci Eng.* <https://doi.org/10.1016/j.petrol.2021.109639>
- MacEachern JA, Pemberton SG (1992) Ichnological aspects of Cretaceous shoreline successions and shoreface variability in the Western Interior seaway of North America. *Application of Ichnology to Petroleum Exploration. SEPMCore Workshop n 17*
- Mianaekere V, Adam J (2020) ‘Halo-kinematic’ sequence-stratigraphic analysis of minibasins in the deep-water contractional province of the Liguro-Provençal basin, Western Mediterranean. *Mar Pet Geol.* <https://doi.org/10.1016/j.marpetgeo.2020.104307>
- Mizutani E, Dreyfus S (2021) On using dynamic programming for time warping in pattern recognition. *Inf Sci* 580:684–704
- Nio S-D (2005) *Climate stratigraphy: principles and applications in subsurface correlation*. EAGE, Houten
- Perez-Muñoz T, Velasco-Hernandez J, Hernandez-Martinez E (2013) Wavelet transform analysis for lithological characteristics identification in siliciclastic oil fields. *J Appl Geophys* 98:298–308
- Qing F, Yan JP, Wang J (2020) Division of sedimentary cycle of sandy conglomerate body and its relationship with physical properties: a case study from the upper submember of the fourth member of Shahejie Formation in Y920 block of northern steep slope zone in Dongying Sag. *Lithol Reserv* 32(6):50–61
- Rivera Vega, N (2004) *Reservoir characterization using wavelet transforms* (Master thesis). Texas A & M University
- Shi B, Cao M, Wang Z, Ostachowicz W (2022) A directional continuous wavelet transform of mode shape for line-type damage detection in plate-type structures. *Mech Syst Signal Process* 167:108510
- Song F, Nina Su, Kong X, Liu C, Song C (2020) Sedimentary characteristics of humid alluvial fan and its control on hydrocarbon accumulation: a case study on the northern margin of the Junggar Basin, west China. *J Pet Sci Eng.* <https://doi.org/10.1016/j.petrol.2019.106729>
- Teama MA, Kassab MA, Cheadle BA, Mesbah MA, Mohamed IF, El-Din ES (2018) 3D seismic and formation micro-imager (FMI) integrated study to delineate depositional pattern of Abu Madi (Upper Miocene) clastic reservoir rocks in El-Wastani gas field, onshore Nile Delta, Egypt. *Egypt J Pet* 27(4):747–758. <https://doi.org/10.1016/j.ejpe.2017.11.003>
- Teixeira L, Lupinacci WM, Maul A (2020) Quantitative seismic-stratigraphic interpretation of the evaporite sequence in the Santos Basin. *Mar Pet Geol.* <https://doi.org/10.1016/j.marpetgeo.2020.104690>

- Wachtmeister H, Höök M (2020) Investment and production dynamics of conventional oil and unconventional tight oil: Implications for oil markets and climate strategies. *Energy Clim Change*. <https://doi.org/10.1016/j.egycc.2020.100010>
- Wang H, Shi Z, Zhao Q, Liu D, Sun S, Guo W, Liang F, Lin C, Wang X (2020) Stratigraphic framework of the Wufeng–Longmaxi shale in and around the Sichuan Basin, China: implications for targeting shale gas. *Energy Geosci* 1(3):124–133. <https://doi.org/10.1016/j.engeos.2020.05.006>
- Weedon GP (2003) Time-series analysis and cyclostratigraphy: examining stratigraphic records of environmental cycles. Cambridge University Press, Cambridge
- Wu W (2020) Seismic sedimentology, facies analyses, and high-quality reservoir predictions in fan deltas: a case study of the Triassic Baikouquan Formation on the western slope of the Mahu Sag in China's Junggar Basin. *Mar Pet Geol* 120:104546
- Xi K (2021) Diagenetic variations with respect to sediment composition and paleo-fluids evolution in conglomerate reservoirs: a case study of the Triassic Baikouquan Formation in Mahu Sag, Junggar Basin, Northwestern China. *J Pet Sci Eng* 197:107943
- Yu Z, Wang Z (2021) Volcanic lithology identification based on parameter-optimized GBDT algorithm: a case study in the Jilin Oilfield, Songliao Basin, NE China. *J Appl Geophys* 194:104443. <https://doi.org/10.1016/j.jappgeo.2021.104443>
- Yu Z, Wang Z, Wang J, Li Z (2022) Subtle reservoirs and implications for hydrocarbon exploration in terrestrial lacustrine fan-delta deposits: Insights from the Triassic Baikouquan Formation, Mahu Sag, Junggar Basin, western China. *Mar Pet Geol*. <https://doi.org/10.1016/j.marpetgeo.2022.105730>

Springer Nature or its licensor (e.g. a society or other partner) holds exclusive rights to this article under a publishing agreement with the author(s) or other rightsholder(s); author self-archiving of the accepted manuscript version of this article is solely governed by the terms of such publishing agreement and applicable law.